Journal Name

ARTICLE

Lysozyme Encapsulated Gold Nanoclusters: Effects of Cluster Synthesis on Natural Protein Characteristics

Received 00th January 20xx,
Accepted 00th January 20xx

DOI: 10.1039/x0xx00000x

www.rsc.org/

B. A. Russell,[a]† B. Jachimska[b] P. Komorek[b,c] P. A. Mulheran[d] and Y. Chen[a]

The study of gold nanoclusters (AuNCs) has seen much interest in recent history due to their unique fluorescent properties and environmentally friendly synthesis method, using proteins as a growth scaffold. The differences in the physicochemical properties of lysozyme encapsulated AuNCs in comparison to natural lysozyme are characterised in order to determine the effects AuNCs has on natural protein behaviour. The molecules hydrodynamic radius (Dynamic Light Scattering), light absorbance (UV-Vis), electrophoretic mobility, relative density, dynamic viscosity, absorption (Quartz Crystal Microbalance) and circular dichroism (CD) characteristics were studied. It was found that lysozyme forms small dimer/trimer aggregates upon the synthesis of AuNCs within the protein. The diameter of Ly-AuNCs was found to be 8.0 nm across a pH range of 2-11 indicating dimer formation, but larger aggregates with diameters >20nm formed between pH 3-6. The formation of larger aggregates limits Ly-AuNCs use as a fluorescent probe in this pH range. A large shift in the protein's isoelectric point was also observed, shifting from 11.0 to 4.0 upon AuNC synthesis. This resulted in major changes to the adsorption characteristics of lysozyme, observed using QCM. A monolayer of 8 nm was seen for Ly-AuNCs at pH 4, offering further evidence the proteins form small aggregates, unlike the natural monomer form of lysozyme. The adsorption of Ly-AuNCs was seen to decrease as pH was increased; this is in major contrast with lysozyme absorption behaviour. A decrease in α-helix content was observed from 25 % in natural lysozyme to 1 % in Ly-AuNCs. This coincided with an increase in β-sheet content after AuNCs synthesis indicating that the natural structure of lysozyme was lost. The formation of protein dimers, the change in protein surface charge from positive to negative, and secondary structure alteration caused by the AuNC synthesis must be considered before attempting to utilise Ly-AuNCs as *in vivo* probes.

Introduction

Protein encapsulated gold nanoclusters (AuNCs) have been shown much interest in recent history due to their unique fluorescent properties[1–3]. Due to their small physical size of less than 2 nm, they show quantum mechanical behaviour; the small number of atoms (2 – 100's) in the clusters results in discrete electronic energy levels, allowing the AuNCs to absorb light and release this energy fluorescently.

Much work has been carried out on the development of methods for the synthesis of AuNCs[4–6]. Of particular interest has been the use of biological molecules to reduce and stabilize gold nanoclusters in a 'one pot' process. It has been shown that the presence of specific amino acid residues and the amount of each in a biological molecule plays a major role in the formation of gold nanoclusters in the one-pot process; however the emission peak in all cases centres in the red regime of the visible spectrum[7]. This method of synthesis has been widely used, using a number of different proteins including; Human Serum Albumin (HSA)[8,9], Bovine Serum Albumin (BSA)[10], Transferrin[11], Trypsin[12], Apo-ferritin[13], Horseradish Peroxidase[14] and Lysozyme[15].

The enzyme, Lysozyme is of particular interest due to the role that it plays in human physiology. It is a relatively small bio-molecule at 14,307 Da in mass, comprising of two domains and a cleft in the protein centre which acts as the active site[16]. The secondary structure of each domain differs significantly, with one domain mainly β-sheet in structure and the other mainly helical[17]. Its main role is to attack the cell walls of bacteria, breaking the cell wall and causing the bacteria to burst under their own internal pressure.[17] Lysozyme AuNCs (Ly-AuNCs) have been shown to make excellent probes for the detection of mercury[15] and glutathione[18], *in vitro* experiments; to date no experiments using Ly-AuNCs *in vivo* as fluorescent probes have been carried out. The functionality of Lysozyme after AuNC synthesis has been shown to still be present to some degree as Liu et. al. successfully showed Ly-AuNCs still possessed good bio recognition for E.Coli[19].

[a] *Department of Physics, Strathclyde University, John Anderson Building, 107 Rottenrow, Glasgow G4 0NG, UK.*
[b] *Jerzy Haber Institute of Catalysis and Surface Chemistry, Polish Academy of Sciences, Niezapominajek 8, 30-239 Cracow, Poland.*
[c] *Faculty of Physics, Astronomy and Applied Computer Science, Jagellonian University,Stanislawa Lojasiewicza, 30-348 Cracow, Poland.*
[d] *Department of Chemical and Process Engineering, Strathclyde University, Glasgow G1 1XJ, UK.*
† Corresponding Author.

A major problem that arises when protein structure changes in human physiology is the formation of large aggregate particles. The misfolding of Lysozyme has been shown to cause the formation of Amyloid fibrils; which have been linked to many human diseases such as Alzheimer's and Parkinson's disease[20–22] due to their insoluble nature. Therefore, it is important to understand how native lysozyme changes upon the nucleation of an AuNC within the protein for any future use of Ly-AuNCs as an in vivo probe. It is also vital to understand any changes to proteins natural characteristics to any future attempts to improve the fluorescence properties of the fluorophore complex.

In this work we applied, electrophoretic mobility[23], QCM-D[24], UV-Vis, density, viscosity[25] and Circular Dichroism (CD) measurement techniques to characterise the physicochemical properties of Lysozyme and Ly-AuNCs under different pH conditions in order to better understand how AuNC nucleation affects Lysozyme's natural state.

Material and Methods

Lysozyme (crystallized and lyophilized powder, from chicken egg white), (≥99%) and Gold(III) Chloride Hydrate were purchased from Sigma Aldrich and used without further purification. A stock solution of Ly-AuNCs was prepared using Wei's *et. al.* method[15] and stored at 4 °C until use, a separate stock of Lysozyme was prepared, dissolving in purified water. The stock solutions were then diluted with NaCl (concentration of I = 10^{-2} M) to a range of concentrations between 5 – 5000 ppm immediately before use. Multiple stock solutions of HCl and NaOH at differing concentrations were used to control the pH of all samples. Doubly distilled, degassed water was used for the preparation of all solutions. All experiments were carried out at 25 °C. All other chemicals used were procured from Sigma-Aldrich.

All Dynamic Light Scattering (DLS) measurements were carried out using a Malvern Zetasizer Nano ZS. The measurement range of the equipment used is 0.6 nm – 0.6 µm. Diffusion coefficients for both lysozyme and Ly-AuNCs were carried out at a concentration of 1000 ppm. The diffusion coefficients were calculated, using equation [1], from the time correlation function which is found by monitoring the changes in intensity of back scattered light from the sample of time as they undergo Brownian motion.

$$g(\tau) = A[1 + Bexp(-2D_{CF}q^2\tau)] \quad [1]$$

Where τ is the sample time, A is the correlation time baseline, B is the correlation function intercept, q is the scattering vector and n is the refractive index of the solution.

Using Stokes' equation [2], the hydrodynamic radii (r_H) can be calculated from the diffusion coefficients and converted to a particle size distribution.

$$r_H = \frac{kT}{(6\pi\eta D_{CF})} \quad [2]$$

Where k is the Boltzmann constant, T is the temperature and η is the solution viscosity.

UV-Vis measurements were carried out using a Perkin Elmer 25. All measurements were carried out at a concentration of 1000 ppm.

Zeta potential measurements were also carried out on the Malvern Zetasizer Nano ZS. The measurement range in the case of measuring electrophoretic mobility is 3 nm – 10 µm. The electrophoretic mobility of lysozyme and Ly-AuNCs was carried out at a concentration of 1000 ppm. Voltages were applied across the same folded capillary cell supplied by Malvern in order to avoid errors associated with cells with differing behaviour. Applied voltages cause charged particles to migrate to the oppositely charged electrodes. During this migration their velocity can be expressed as the electrophoretic mobility (μ_e). Using Henry's equation [3] the zeta potential of the samples were found.

$$\xi = \frac{3\eta}{2\varepsilon F(\kappa a)\mu_e} \quad [3]$$

Where ξ is the zeta potential, ε is the dielectric constant of water, F(κa) is the function of the dimensionless parameter κa.

Density measurements were carried out using an Anton Paar DMA 5000M digital vibrating U-tube densimeter (precise to within 5 x 10^{-6} gcm^{-3}). Viscosity measurements were carried out using an Anton Paar ME rolling ball microviscometer (precise to within 0.001 s). The density and viscosity of lysozyme and Ly-AuNCs was measured over a range of 0 – 5000 ppm. All dilutions were carried out using degassed NaCl (I = 1 x 10^{-2}).

Quartz Crystal Microbalance(QCM) measurements were carried out using a Q-Sense E1 QCM-D. Sensors with gold electrode surfaces were used for all experiments. A constant flow speed of 500 µl/min was used throughout the experiment. Initially NaCl solution was passed over the sensor for 10 minutes in order to set a baseline for the adsorption. The sample solution was then passed over for 90 minutes at a concentration of 5 ppm and pH range of 4 – 10, during which time the adsorption was monitored. NaCl was then rinsed over the gold surface for another 90 minutes in order to observe whether the adsorption of protein to the gold surface was irreversible. Before each measurement the sensor was cleaned using the same protocol each time.

The Sauerbrey model was utilized in order to correlate changes to the frequency at which the quartz crystal resonated at to the mass of protein adsorbed to the sensor surface[26]. When adsorption occurs on the sensors' electrode surface the total mass increases, causing the resonant frequency (f) decrease. For rigid, uniform films the decrease in resonant frequency ($\Delta f = f - f_0$), is directly proportional to the adsorbed mass (Γ_{AD}), as shown in equation [4].

$$\Gamma_{AD} = -C\frac{\Delta f}{n} \quad [4]$$

Where C is the crystal constant for quartz (equal to 17.7 ngcm^2) and n is the overtone number.

From knowing the Sauerbrey mass adsorbed to the sensor surface it is possible to calculate the effective thickness layer (d_{eff}) if the density of the layer is known. In this case the density value has been previously calculated and given as 1330 kgm^{-3} [27]. The thickness can then be calculated using the following equation [5].

$$d_{eff} = \frac{\Gamma_{AD}}{\rho_{eff}} \quad [5]$$

Where ρ_{eff} is the effective density of the layer.

Circular Dichroism (CD) measurements were carried out using a Jasco J-1500 spectrometer. Solvent baseline measurements were taken using NaCl (I = 10^{-2} M) before the CD spectra of lysozyme and Ly-AuNCs at different pH were acquired. The concentration of lysozyme and Ly-AuNCs was kept at a concentration 50 ppm. Spectra were recorded over a range of 185-300 nm with a scan speed of 50 nm/min and a bandwidth of 1 nm using a quartz cuvette with a path length of 0.1 cm.

Results

Initially the hydrodynamic radius, r_H was determined for both lysozyme and Ly-AuNCs as a function of pH, across a pH range of 2-11, at a sample concentration of 1000 ppm. The radius for each sample was calculated from the diffusion coefficient of the measured sample using the DLS technique. The determined diameters for Lysozyme and Ly-AuNCs are shown in Figure 1. The hydrodynamic diameter by volume of Lysozyme was found to be 4.0 nm, between pH 4-10. The diameter of Lysozyme compares well with previous studies[28,29] and is stable at lower pH due to the smaller, more robust nature of the protein. The diameter of Ly-AuNCs was found to be significantly higher at 8.0 nm across the pH range, comparing well with previous studies carried out[30]. This suggests that the proteins are forming dimers or tightly packed trimers upon the synthesis of AuNCs. Between pH 3-5 the diameter of Ly-AuNCs was found to be greater than 20 nm and polydisperse, indicating the formation of large aggregates. The aggregation of protein encapsulated AuNCs at this pH has previously been observed, suggesting that the presence of AuNCs within the protein is directly responsible. The formation of protein aggregates after AuNC synthesis in lysozyme has previously been detected by T. Pradeep *et. al.* via mass spectroscopy; agreeing with our findings[31]. The aggregation was also seen to be reversible by lowering or increasing the pH above or below the window of aggregation, indicating that no irreversible bonding between the lysozyme proteins takes place.

UV-Vis absorption spectroscopy measurements were taken of both Lysozyme and Ly-AuNCs under the same conditions as the DLS measurements shown previously, shown in Figure 2.

The absorption of Lysozyme can be seen slowly increasing as the pH approaches the isoelectric point at pH 11.0.The absorption of Ly-AuNCs is seen to be much higher across the whole pH range, due to the presence of the AuNCs. Between pH 3-6 the absorption of Ly-AuNCs increases dramatically, peaking around pH 4. This large increase coincides with a change in colour from clear to cloudy and also matches the pH range at which aggregation of Ly-AuNCs was seen from DLS experiments, confirming the previous result. This result agrees well with the pH induced aggregation of HSA-AuNCs previously reported[32].The electrophoretic mobility of both Lysozyme and Ly-AuNCs was measured across a pH range of 3-11, at a concentration of 1000 ppm in both cases. The associated zeta potentials were calculated using Henry's equation, [3], and displayed in Figure 3.

The zeta potential curve for Lysozyme in a solution with ionic strength I = 1 x 10^{-2} M compares well with previously published results[33].The isoelectric point of Lysozyme in this case is approximately 10.0, in agreement with previous results[26]. In the case of lysozyme AuNC nucleation dramatically changes the zeta potential. From pH 5.0 to 11.0, there is a significant difference between lysozyme and Ly-AuNCs equal to 50 mV. Additionally the shift in isoelectric point changes from 10.0 to 4.0. The zeta potentials across the pH range of Ly-AuNCs were found to be remarkably different. Between pH 3-6 the surface charge of Ly-AuNCs was seen to drop rapidly from 40 mV to -40 mV. After pH 6 the surface charge was seen to continue to decrease at a lower rate, dropping to -60 mV at pH 11. The

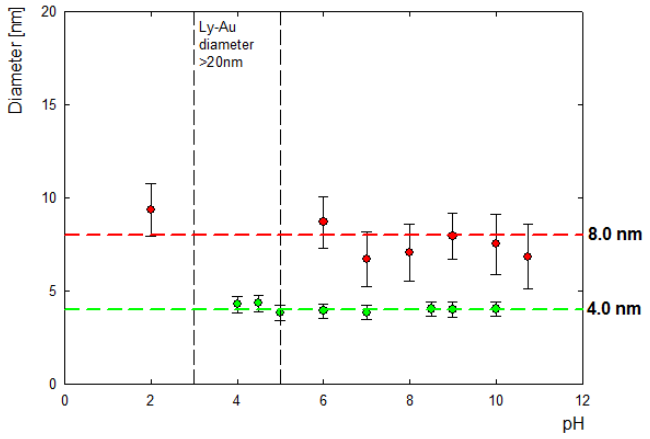

Figure 1: Hydrodynamic diameter of Lysozyme (green) and Ly-AuNCs (red) as a function of pH. For the pH range 3-5 Ly-AuNCs diameter are >20nm and polydisperse.

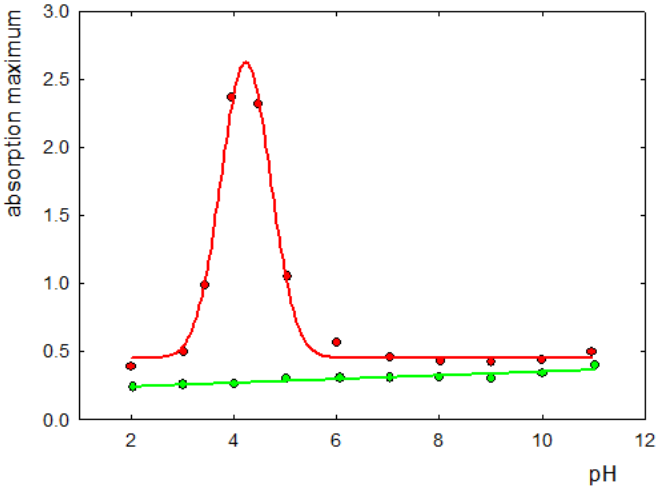

Figure 2: Maximum UV-Vis absorption of Ly-AuNCs (red) and Lysozyme (green) at 300nm as a function of pH.

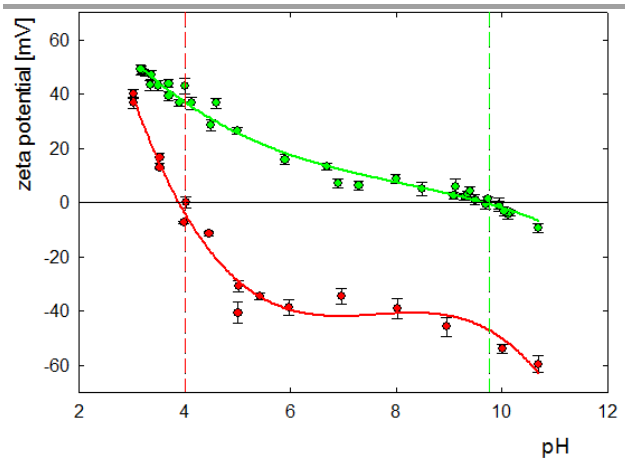

Figure 3: Zeta potential of Lysozyme and Ly-AuNCs as a function of pH. The zeta potentials of Lysozyme and Ly-AuNCs are indicated in green and red respectively.

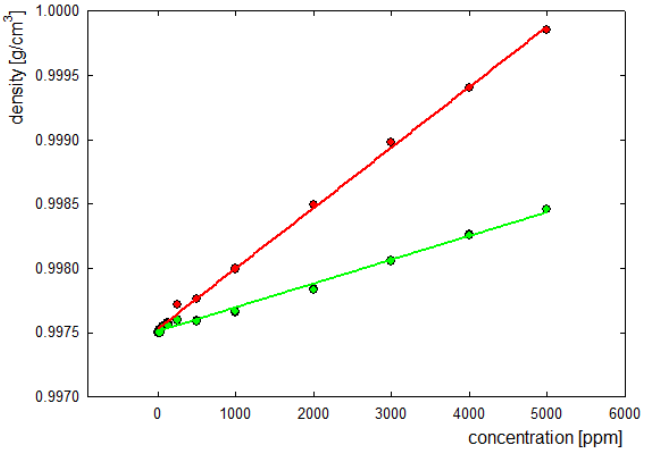

Figure 4: Lysozyme and Ly-AuNCs density as a function of concentration are shown. The density of lysozyme is represented by green while Ly-AuNCs density is represented by red.

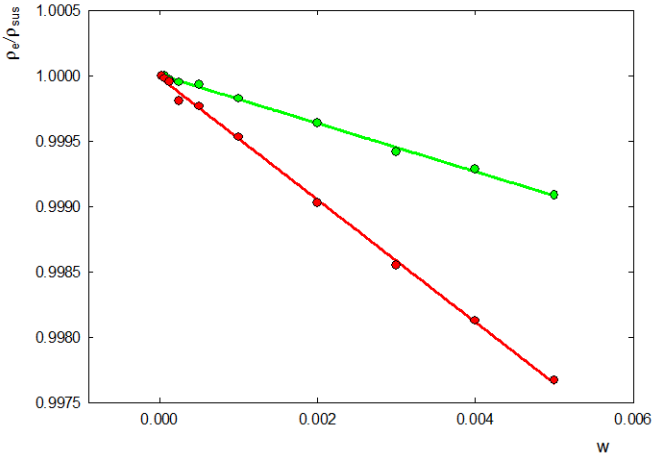

Figure 5: Relative density of lysozyme and Ly-AuNCs as a function of weighted fraction. The relative density gradient of lysozyme is shown in green while the relative density gradient of Ly-AuNCs is shown in red. The gradients for lysozyme and Lysozyme-AuNCs were found to be -0.1985 and -0.4680 respectively; this gave lysozyme a relative density of 1.33 while Ly-AuNCs had a relative density of 1.87.

major changes to the zeta potential profile of Ly-AuNCs can be directly attributed to either the presence of the AuNCs or unreacted gold salt still attached to the protein surface[28]. The isoelectric point of Ly-AuNCs is similar to that of HSA-AuNCs, suggesting that the nucleation of AuNCs within proteins may result in the shifting of the complexes isoelectric point to around 4.0, regardless of the proteins natural isoelectric point. Ly-AuNCs maximum aggregation takes place at the same pH as the isoelectric point suggesting that the proteins reversibly aggregation with no repulsive surface charge to separate them. This could have major implications of using protein encapsulated AuNCs in any situation where the pH of the environment being imaged or probed is close to this protein-AuNC critical isoelectric value. Another factor which must be addressed is the change from a positive surface charge for natural lysozyme to a negatively charged surface for Ly-AuNCs at body pH (7.4). The zeta potential decreases from 17 mV to -35 mV. The net positive charge of the lysozyme protein has been reported to play an important role in the initiation of its lytic action and indeed its efficiency against the negatively charged cell walls of certain bacteria[34].This result therefore raises questions to lysozyme's ability to function correctly after the synthesis of AuNCs.

The density of lysozyme and Ly-AuNCs was measured across a concentration range of 0 - 5000 ppm which was diluted from stock using degassed NaCl solution (I = 1 x 10^{-2}). The difference between lysozyme and Ly-AuNCs density is shown in Figure 4. The density of Ly-AuNCs is seen to be higher than Lysozyme due to the extra mass the presence of the AuNCs adds to the lysozyme protein. In order to properly quantify the increase in relative density the AuNCs have on the lysozyme protein, the values from Figure 4 were converted to relative density values and shown in Figure 5.

The relative density of a material can be described as the ratio of the density of a substance to that of the reference solvent[35], in this NaCl used to dilute the lysozyme and Ly-AuNCs. For lysozyme a relative density value of 1.33 gcm^{-3} was calculated, matching the previously reported value of 1.33 gcm^{-3} for proteins[27]. The relative density of Ly-AuNCs was found to be far in excess of the normal protein relative density, at a value of 1.87 gcm^{-3}. This increase in relative density upon synthesising AuNCs within lysozyme is even greater than the increase seen for HSA-AuNCs[28]. The only possible reason for the increase can only be attributed to the mass of AuNCs and possible excess gold salt attached to the protein surface, since no other molecules were introduced to the samples after synthesis and dilution. All positively charged residues that make up the lysozyme primary structure are located on the protein surface. This gives the protein a highly positive surface charge making it likely that negatively charged chloride ions created as a result of the gold salt reduction are bound to the protein surface.

The increase in density between lysozyme and Ly-AuNCs is 0.54 gcm^{-3}. Attributing this value solely to the mass of gold, we can find that the average amount of gold atoms per lysozyme

protein is 29 atoms. If every lysozyme present has an encapsulated AuNC then this value is close to the expected number of atoms within red emitting AuNCs at 25 atoms.

The increase in amount of gold per lysozyme can be attributed again to unreacted gold salt on the protein surface, or it is possible that in some lysozyme smaller, AuNC intermediate products have formed which contain less gold atoms and are not fluorescent. Combining the molecular weights of Lysozyme and the added weight assuming it is that of the AuNCs then we can estimate that the molecular weight of Ly-AuNCs is 20020 Da.

The dynamic viscosity of lysozyme and Ly-AuNCs was measured over a concentration range of 0 - 5000 ppm in order to study the effects of the aggregation seen in previous experiments. From Figure 6 it can be seen that the viscosity of Ly-AuNCs is considerably higher than that of lysozyme. The higher viscosity of Ly-AuNCs than that of natural lysozyme is unsurprising. This observation can be explained by the formation of dimers seen previously from the DLS experiment. In both cases the increase in viscosity in respect to the concentration was seen to be linear, suggesting that while the Ly-AuNCs viscosity is higher, it doesn't reach a critical viscosity at which the protein complex no longer flows in solution. The increase in viscosity for Ly-AuNCs can be attributed to a decrease in the rate of diffusion which arises due to the higher hydrodynamic radius of Ly-AuNCs.

The adsorption of lysozyme and Ly-AuNCs to a gold surface was studied as a function of pH using QCM-D. A pH range of 4-10 was used in both cases at a constant sample concentration of 5 ppm. It was found that the presence of AuNCs had a major effect on the adsorption mass of Ly-AuNCs at different pH in comparison to natural lysozyme, shown in Figure 7.

The adsorption maxima for lysozyme and Ly-AuNCs are seen to be remarkably different. The adsorption maximum was found to be 900 ngcm^{-2} at pH 4 for Ly-AuNCs while the adsorption maximum for lysozyme was found to be 450 ngcm^{-2} at pH 10. The adsorption maxima in both cases occur at the isoelectric point for each molecule. Between pH 5.0 – 10.0 the adsorbed mass is seen to be relatively the same. The higher adsorption of Ly-AuNCs at pH 4.0 can be attributed to aggregation effects earlier observed at this pH. The effectiveness of adsorption in both cases is directly linked to the overall magnitude of the charge, with the larger charge resulting in less effective adsorption. However, it is important to note that the polarity of the charge does not seem to be important for the adsorption to the gold surface to take place. This can be more effectively visualised by plotting the overall mass adsorbed in each case against the zeta potential, as shown in Figure 8.

To better understand the effect of AuNCs on the adsorption of lysozyme the thickness of the adsorption layer formed on the gold surface was calculated from the mass adsorbed and the known densities of both lysozyme and Ly-AuNCs using Equation [5]. The results are shown in Figure 9. It can be seen across the pH range that lysozyme forms layers with thicknesses between 2-4 nm. Ly-AuNCs can be seen to form layers with a much wider range of thicknesses from 1-8 nm. It

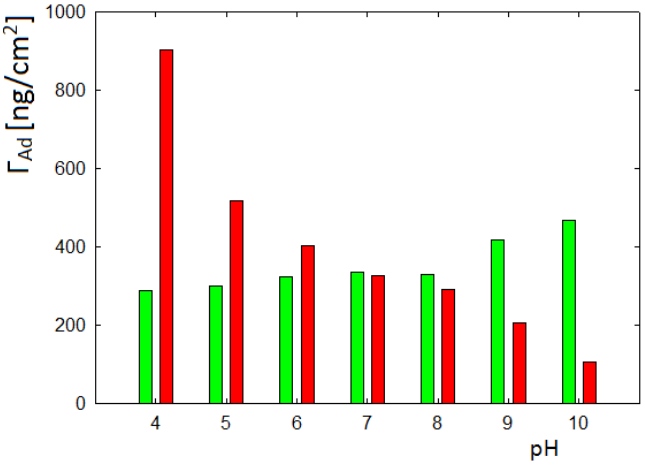

Figure 7: The mass of adsorbed molecules per geometrical unit of the gold surface, Γ_{Ad} [ngcm^{-2}], as a function of pH is shown. The result for lysozyme is shown in green while Ly-AuNCs are displayed in red.

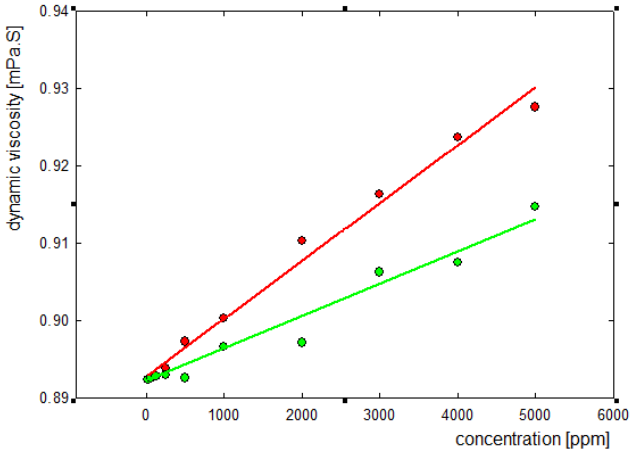

Figure 6: Dynamic viscosity of lysozyme and Ly-AuNCs as a function of concentration. The dynamic viscosity values for lysozyme are shown in green while Ly-AuNCs viscosity is shown in red.

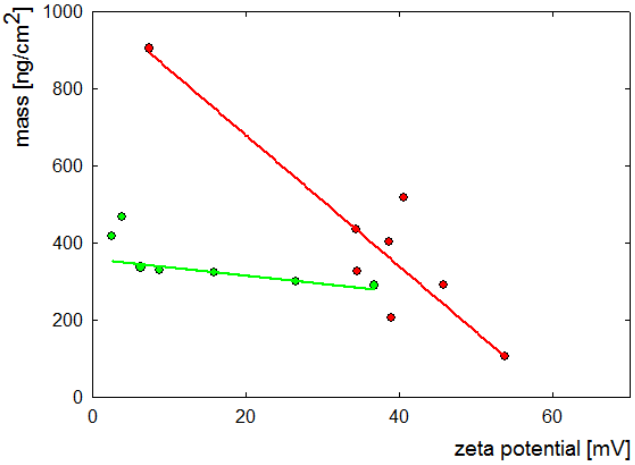

Figure 8: The mass of adsorbed molecules per geometrical unit of the gold surface, Γ_{Ad} [ngcm^{-2}], as a function of zeta potential magnitude is shown. The result for lysozyme is shown in green while Ly-AuNCs are displayed in red.

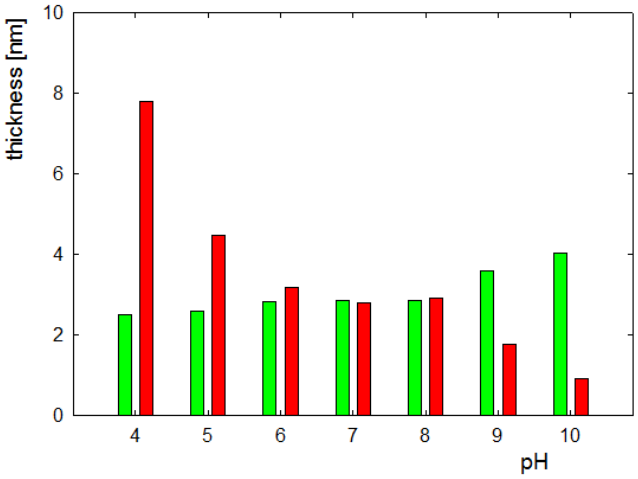

Figure 9: The thickness of the adsorbed layer as a function of pH on a gold surface is shown. The thickness of the lysozyme adsorption layer is shown in green while the thickness of Ly-AuNCs is shown in red.

is observed that the further from the molecules isoelectric point, the smaller the total mass adsorbed and the layer thickness, suggesting that the proteins at different pH contact and adsorb to the gold at different angles, with lower surface coverage being observed at lower layer thicknesses. In both cases the maximum thickness layer is equal to the hydrodynamic diameter found during the DLS experiments previous. The QCM-D result therefore suggests that at the isoelectric point in each case the proteins form closely packed monolayers, with the proteins in a geometry that has a minimal amount of contact with the gold surface. This again suggests that the Ly-AuNCs exist in a small aggregated form, resulting in the thicker monolayer in comparison with natural lysozyme. This result bodes well for the utilisation of Ly-AuNCs at body pH (7.4) as the adsorption behaviour of Ly-AuNCs and lysozyme have been seen to be similar in regards to total mass and thickness of monolayers adsorbed to a surface and while dimers have been seen from previous experiments, they do not negatively affect the proteins adsorption behaviour at neutral pH.

The lysozyme protein has a tertiary structure comprised of two domains, as shown in Figure 10. The first domain is highly alpha helical, made up of 4 alpha helices while the second is made up of 3 beta sheets. Previous CD measurements carried out by Chang *et. al.* have shown the total alpha helix content of lysozyme to be 30 % while the beta sheet content is 35 %[36]. The CD spectrum in the far-UV region (190−250 nm) is used to probe the secondary structure, conformation, and stability of proteins in solution[35]. Thus, it is an important spectroscopic tool for the quantification of the conformational changes of lysozyme after AuNC nucleation. Two negative bands characteristic of the typical α-helix structure of protein were observed in the CD spectra of lysozyme at 208 and 220 nm in the ultraviolet region. The negative peaks at 208 and 220 nm correspond to the $\pi \rightarrow \pi^*$ and $n \rightarrow \pi^*$ transition due to the peptide bond of an α-helix[37]. The CD spectrum of native lysozyme and Ly-AuNCs are shown in Figure 11. The estimated

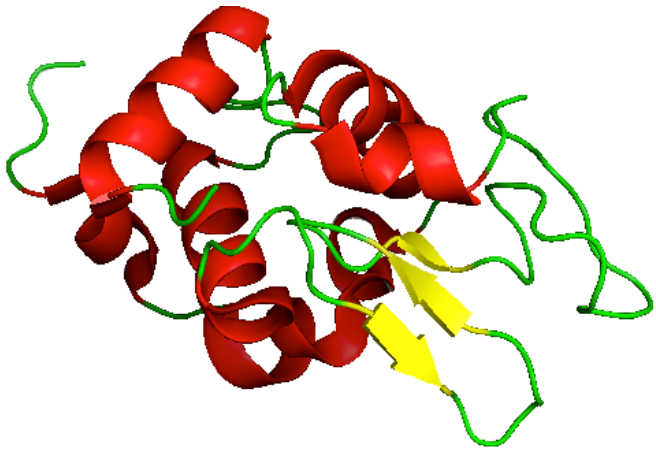

Figure 10: Structure of Lysozyme protein. The protein is comprised of two domains; one which is mostly alpha helical in nature and the other consists of mainly beta sheet formations. Alpha-helices are shown in red, beta sheets are shown in yellow and turns are shown in green.

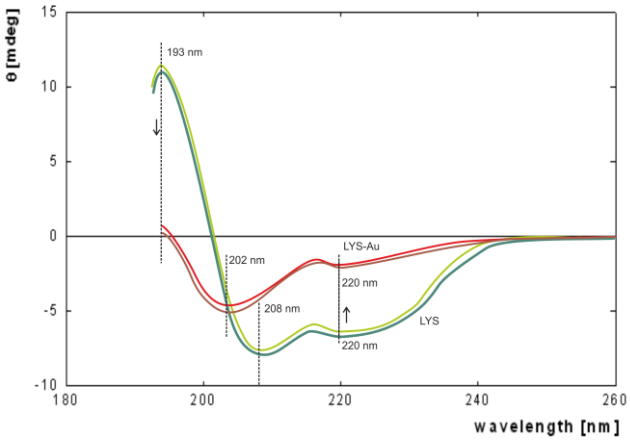

Figure 11: CD spectra of lysozyme and Ly-AuNCs at different pH. Ly-AuNCs at pH 5.5 is shown in red, Ly-AuNCs at pH 7.5 is shown in brown, lysozyme at pH 5.5 is shown in light green and lysozyme at pH 7.5 is shown in dark green.

α-helicity content of native lysozyme in NaCl solution (pH 7.40 and at T = 298 K) comes out to be 25%, which agrees reasonably with literature reports[36]. The intensity of α-helix peaks show a gradual declination with addition gold. The % of the helical content changes from 25 to 1 at pH 7.5 as shown in Table 1.

Figure 11 shows that the intensity of the α-helix peak of peptide near 208 nm decreased after formation complex with gold. The changes to the structure of lysozyme can be attributed to the nucleation of AuNCs.

The largest changes were observed as a 24 % decrease in α-helix content and 15 % increase in β-sheet content after AuNCs synthesis. Changes in the lysozyme CD spectrum suggest that the interactions between these molecules are complex and causes multidirectional alterations in the protein structure. The percentage makeup of the protein before and after AuNC synthesis is shown in Table 1.

	Lysozyme	Ly-AuNCs
α-helix (%)	25.7	1.0
β-sheet (%)	41.1	55.9
Turn (%)	1.2	0.8
Random (%)	32.0	42.3

Table 1: Secondary structures present in lysozyme and Ly-AuNCs as a percentage of total secondary structure content.

Typical electron excitation in organic compounds relate to π → π * and n → π*. In the case of the transition π → π *, an increase in the polarity of the environment causes the band shift towards longer wavelengths. This conversely results in an → π * transition. The minimum observed at 220 nm shifts towards lower wavelengths. This can be attributed to a gradual increase in the content of disordered structures in the studied systems.

Conclusions

Important changes to the physicochemical characteristics of lysozyme upon the synthesis of AuNCs using the one-pot method to grow the AuNC within the protein have been observed. Lysozyme was seen to form small aggregates of dimer/trimer size upon the nucleation of AuNCs within the protein. These aggregates were seen to be present across a pH range of 2-11 and larger reversible aggregation of the Ly-AuNCs was observed between pH 3-6. The reversible larger aggregates were confirmed to form due to the massive shift in the isoelectric point of lysozyme from 10.0 to 4.0. This shift has been directly attributed to the formation of AuNCs within the protein. Viscosity and density measurements of both lysozyme and Ly-AuNCs suggested the formation of aggregates also. QCM-D measurements of both Ly-AuNCs and lysozyme unveiled significant differences in the adsorption behaviour of both molecules. The maximum adsorptions of Lysozyme and Ly-AuNCs were found to take place at pH 10 and pH 4, respectively, explained by the massive shift in isoelectric point. The adsorption mass and layer thickness at neutral pH however was found to be near identical. CD data suggests that the AuNCs nucleation within lysozyme denatures the protein to a large factor. The changes to protein surface charge, the formation of protein dimers upon AuNCs synthesis and changes to the protein secondary structure must be taken into account when using AuNCs as a label for observing protein behaviour, however there is still much scope for the Ly-AuNCs fluorophore to be used in sensing and imaging if these changes to the natural protein characteristics are taken into account.

Acknowledgements

Ben A. Russell would like to acknowledge the ERASMUS+ mobility project for funding the research visit to the Jerzy Haber Institute of Catalysis and Surface Chemistry PAS in Cracow, Poland. This work was supported by Grant NCN OPUS 2012/07/B/ST5/00767. Ben A. Russell would also like to acknowledge Karolina Tokarczyk, Monika Cwieka and Sylwia Swiatek for their help in the preparation of all other experimental procedures carried out.

Notes and references

1 C. J. Lin, T. Yang, C. Lee, S. H. Huang and R. A. Sperling, 2009, **3**, 395–401.
2 L. Shang, S. Dong and G. U. Nienhaus, *Nano Today*, 2011, **6**, 401–418.
3 H. Kawasaki, K. Hamaguchi, I. Osaka and R. Arakawa, *Adv. Funct. Mater.*, 2011, **21**, 3508–3515.
4 Y. Lu and W. Chen, *Chem. Soc. Rev.*, 2012, **41**, 3594–3623.
5 B. Yuping, Z. Chang, D. M. Vu, J. P. Temirov, R. B. Dyer and J. S. Martinez, *J. Phys. Chem. C*, 2007, **111**, 12194–12198.
6 X. Tu, W. Chen and X. Guo, *Nanotechnology*, 2011, **22**, 095701.
7 Y. Xu, J. Sherwood, Y. Qin, D. Crowley, M. Bonizzoni and Y. Bao, *Nanoscale*, 2014, **6**, 1515–24.
8 B. A. Russell, K. Kubiak-Ossowska, P. A. Mulheran, D. J. S. Birch and Y. Chen, *Phys. Chem. Chem. Phys.*, 2015, **17**, 21935-21941.
9 B. A. Russell, P. A. Mulheran, D. J. S. Birch and Y. Chen, *Phys. Chem. Chem. Phys.*, 2016, **18**, 22874-22878.
10 J. Xie, Y. Zheng and J. Y. Ying, *J. Am. Chem. Soc.*, 2009, **131**, 888–889.
11 X. Le Guével, N. Daum and M. Schneider, *Nanotechnology*, 2011, **22**, 275103.
12 J. M. Liu, J. T. Chen and X. P. Yan, *Anal. Chem.*, 2013, **85**, 3238–3245.
13 C. Sun, H. Yang, Y. Yuan, X. Tian, L. Wang, Y. Guo, L. Xu, J. Lei, N. Gao, G. J. Anderson, X.-J. Liang, C. Chen, Y. Zhao and G. Nie, *J. Am. Chem. Soc.*, 2011, **133**, 8617–24.
14 F. Wen, Y. Dong, L. Feng, S. Wang, S. Zhang and X. Zhang, *Anal. Chem.*, 2011, **83**, 1193–6.
15 H. Wei, Z. Wang, L. Yang, S. Tian, C. Hou and Y. Lu, *Analyst*, 2010, **135**, 1406–1410.
16 R. E. Canfield, *J. Biol. Chem.*, 1963, **228**, 2698–2707.
17 V. Tullio, S. Roberta and P. Manuela, *Hum. Mosq. Lysozymes Old Mol. New Approaches Against Malar.*, 2015, **35**, 45–57.
18 T. H. Chen and W. L. Tseng, *Small*, 2012, **8**, 1912–1919.
19 J. Liu, L. Lu, S. Xu and L. Wang, *Talanta*, 2015, **134**, 54–59.
20 C. M. Dobson, *Philos. Trans. R. Soc. Lond. B. Biol. Sci.*, 2001, **356**, 133–45.
21 D. R. Booth, M. Sunde, V. Bellotti, C. V Robinson, W. L. Hutchinson, P. E. Fraser, P. N. Hawkins, C. M. Dobson, S. E. Radford, C. C. Blake and M. B. Pepys, *Nature*, 1997, 385, 787–793.
22 J. Raab, F. Haupt, M. Scholz, C. Matzke, K. Warncke, K. Lange, R. Assfalg, K. Weininger, S. Wittich, S. Lobner, A. Beyerlein, U. Nennstiel-Ratzel, M. Lang, O. Laub, D. Dunstheimer, E. Bonifacio, P. Achenbach, C. Winkler and A.-G. Ziegler, *BMJ Open*, 2016, **6**, 011144.
23 B. Jachimska, A. Kozłowska and A. Pajor-Świerzy, *Langmuir*, 2012, **28**, 11502–11510.
24 B. Jachimska and a. Pajor, *Bioelectrochemistry*, 2012, **87**, 138–146.

25 B. Jachimska and Z. Adamczyk, *J. Eur. Ceram. Soc.*, 2007, **27**, 2209–2215.
26 B. Jachimska, K. Tokarczyk, M. Łapczyńska, A. Puciul-Malinowska and S. Zapotoczny, *Colloids Surfaces A Physicochem. Eng. Asp.*, 2016, **489**, 163–172.
27 J. Tsai, R. Taylor, C. Chothia and M. Gerstein, *J. Mol. Biol.*, 1999, **290**, 253–66.
28 J. M. Bezemer, D. W. Grijpma, P. J. Dijkstra, C. A. Van Blitterswijk and J. Feijen, *J. Control. Release*, 1999, **62**, 393–405.
29 A. Valstar, W. Brown and M. Almgren, *Langmuir*, 1999, **15**, 2366–2374.
30 Y. H. Lin and W. L. Tseng, *Anal. Chem.*, 2010, **82**, 9194-9200.
31 A. Baksi, P. L. Xavier, K. Chaudhari, N. Goswami, S. K. Pal and T. Pradeep, *Nanoscale*, 2013, **5**, 2009-2015.
32 B. A. Russell, B. Jachimska, I. Kralka, P. A. Mulheran and Y. Chen, *J. Mater. Chem. B*, 2016, **4**, 6876–6882.
33 K. Kubiak-ossowska, B. Jachimska and P. A. Mulheran, *Phys. Chem. Chem. Phys.*, 2015, **17**, 1–20.
34 H. R. Ibrahim, A. Kato and K. Kobayashi, *J. Agric. Food Chem.*, 1991, **39**, 2077–2082.
35 J. Vörös, *Biophys. J.*, 2004, **87**, 553–61.
36 S. W. Provencher and J. Glöckner, *Biochemistry*, 1981, **20**, 33–37.
37 N. J. Greenfield, *Nat. Protoc.*, 2006, **1**, 2876–2890.